ELSEVIER

PII: S0032-3861(98)00091-3

Polymer Vol. 39 No. 26, pp. 6969–6975, 1998

0032-3861/98/$ - see front matter

Mechanisms of ionic conductivity for zwitterionic polymers

J.H. Pérez[a], J. Cardoso[b] and O. Manero[c,*]
[a]*Departamento de Ingeniería Química, Universidad de Guadalajara, Boul. M. García Barragán, #1451, Guadalajara, Jal. 44430, Mexico*
[b]*Departamento de Física, Universidad Autónoma Metropolitana, A.P. 55-534, México DF 09340, Mexico*
[c]*Departamento de Polímeros, Instituto de Investigaciones en Materiales, UNAM, AP 70-360, México DF 04510, Mexico*
(Received 21 August 1997; revised 14 November 1997; accepted 16 December 1997)

In this work, ionic conductivity data of zwitterionic polymers are compared with predictions of the random free-energy barrier model for a.c. conduction in disordered solids. It is shown that conductivity follows a long range delocalized diffusion of charge carriers within an equally probable distribution of free-energy barriers. Accordingly, it follows time–temperature superposition, expressed as a master curve for the normalized conductivity as a function of the non-dimensional frequency. The dielectric behaviour is dominated by ionic conductivity, and results suggest a process of quasi-ideal conduction of the ion carriers, consistent with a large value of the dielectric relaxation time characteristic of delocalized conduction processes. It is further remarked that alternative interpretations to the conduction behaviour in these polymers can also be given by other theories and models.

(Keywords: zwitterionic polymers; ionic conductivity; conducting polymers)

INTRODUCTION

Ionic conductivity mechanisms in polymers bear similarities to those of ceramics and disordered solids. In general, at low frequencies a constant ionic conductivity (d.c.) is observed, while at higher frequencies the conductivity becomes frequency dependent (a.c.), and it varies approximately as a power of the frequency. A strong temperature dependence (i.e. Arrhenius) d.c. conductivity is observed, while the a.c. conductivity depends weakly on temperature.

A wealth of models have been proposed to account for the observed frequency dependent a.c. conduction. Based on the fact that over a specific frequency interval conductivity is an increasing function of frequency, some models have considered the process of thermally activated hopping across an energy barrier to explain such behaviour. Other models suggest that a.c. and d.c. conduction are due to the same mechanism[1].

The frequency-dependent ionic conductivity strongly suggests that any model for a.c. conduction should be built on the assumption of a distribution of energy barriers. The simplest possible assumption is that all free-energy barriers are equally likely. Indeed, Dyre[2] has suggested a model which assumes that conduction takes place by hopping, where the hopping charge carriers are subjected to spatially randomly varying energy barriers. To calculate the conductivity in random media the model considers the simplest possible nontrivial mean-field approximation, i.e., the continuous time random walk approximation[3]. This approximation may be represented by an equivalent electrical circuit in which the capacitances are equal while the resistances may vary. In this case, the impedance $Z(\omega)$ is given by

$$Z(\omega) = \langle 1/(R^{-1} + i\omega C) \rangle, \tag{1}$$

where C is the capacitance and the average is taken over the distribution of resistances R. Corresponding to the randomly varying free-energy barriers, the resistance probability distribution varies as R^{-1}, and thus the characteristic time $t = RC$ is distributed according to t^{-1}. Equation (1) becomes:

$$Z(\omega) = \frac{K}{C} \int_0^{\tau} \frac{1}{t^{-1} + i\omega} \frac{\mathrm{d}t}{t} = \frac{K}{C} \int_0^{\tau} \frac{1}{1 + i\omega t} \mathrm{d}t \tag{2}$$

where τ is the relaxation time. K is a constant which is determined self-consistently. Solution of equation (2) gives the following expression for the conductivity:

$$\sigma(\omega) = \sigma_0 \frac{i\omega\tau}{\ln(1 + i\omega\tau)}. \tag{3}$$

Note that the integral in equation (2) assumes an equal distribution of relaxation times τ, which is consistent with the hypothesis of equally likely free-energy barriers.

The random free-energy barrier model predicts an universal shape of the conductivity curve, when the reduced conductivity is plotted with dimensionless frequency in a log–log graph. The model implies a high-frequency behaviour which is very close to a power law, with exponents ranging between 0.7 and 1.0, as observed experimentally. Results of a.c. conductivity allow for a detailed discussion of possible mechanisms of charge transport.

In this work, ionic conductivity data of a class of ionic polymers, i.e., zwitterionic moieties, are compared with predictions of the random free-energy barrier model for a.c.

* To whom correspondence should be addressed

conduction in disordered solids. Agreement with predictions from equation (3) is highlighted. In addition, it is shown that these polymers present relaxation mechanisms characteristic of a delocalized conduction process, or quasi-ideal conduction. Conductivity follows a long range delocalized diffusion of charge carriers within an equally probable distribution of free-energy barriers.

EXPERIMENTAL PART

The polymer synthesis was performed through a quaternization reaction with butane–sultone on the precursor polymer, according to the technique described elsewhere[4]. Copolymers with a specific ionic content are obtained, and the ionic groups are randomly distributed along the polymer chain. The resulting molecular structure is the following:

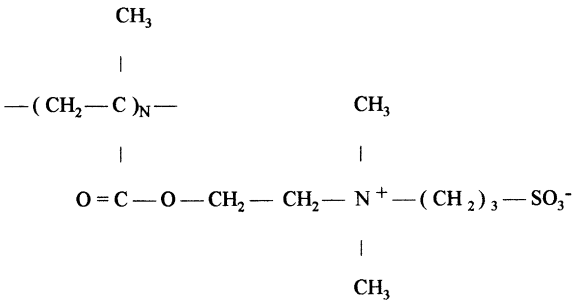

Molecular weights of the precursor polymer were determined by light scattering in a Wyatt Down-F apparatus. Quantitative analysis of the ionic groups was made by elemental analysis. Average molecular weights of the precursor polymer (1.2×10^5) and of the quaternized copolymer (2.1×10^5), with a 80.5% of ionic groups, were determined. Subsequent characterization of the resulting copolymer was obtained by *FT*-i.r. (Perkin Elmer 1600), d.s.c. and t.g.a. (TA Instruments, DSC 9105 and TGA 951).

FT-i.r. identified the bands corresponding to the quaternized nitrogen (1790 cm^{-1}) and those of the sulfonate group (1384 and 1180 cm^{-1}). The glass transition temperature of the polymer is 141.5°C. Due to the high hygroscopicity of the samples, it was necessary to undertake a thermal treatment before measurements. A weight loss of 8.3% at 104°C was found due to water evaporation. Decomposition of the lateral groups and main chain take place at 270 and 366°C, respectively.

Dielectric spectroscopy measurements required disk-shaped samples with 25.4 mm. diameter. These were shaped from powder samples by pressing them using a hydraulic press (Carver-C) under vacuum and a dryer. Two gold-folded electrodes were used with a dielectric analyser (DEA-2970, TA Instruments) equipped with a Wegner bridge coupled to a TA-2100 console. Measurements were taken from 170°C up to 240°C under inert atmosphere provided by a nitrogen flow of 500 cc/min. The procedure to perform the tests included an initial step increment of 2–3°C in temperature and 5 min equilibration time. A frequency sweep of 21 frequencies (between 0.1 Hz and 0.3 MHz) was carried out at constant temperature during 3 min sample time. Thereafter, a further step increment in temperature is made and the procedure above is repeated up to the maximum temperature (240°C). Finally, the sample is removed from the electrodes using trifluoroethanol and acetone.

RESULTS

Since the conductivity measurements require that the powder samples be compacted under pressure, conductivity was measured on samples conformed under several compacting pressures. Results indicate that the conductivity is a function of the compacting pressure, phenomena which has been given particular attention recently[5]. Analysis of data was carried out on samples which presented the maximum conductivity, which corresponds to a compacting pressure of 6 ton/cm^2 ($\approx 6 \times 10^8$Pa).

Data analysis and presentation may be made in several ways: using the dielectric constant

$$\varepsilon(\omega) = \varepsilon'(\omega) - \varepsilon''(\omega)i, \tag{4}$$

or the conductivity

$$\sigma(\omega) = \sigma'(\omega) + \sigma''(\omega)i. \tag{5}$$

These two quantities are related by

$$\varepsilon_0 \varepsilon(\omega) = [\sigma(\omega) - \sigma(0)]/i\omega, \tag{6}$$

where ε_0 is the vacuum permittivity. Alternatively, in ionic conduction is sometimes preferred to present data in terms

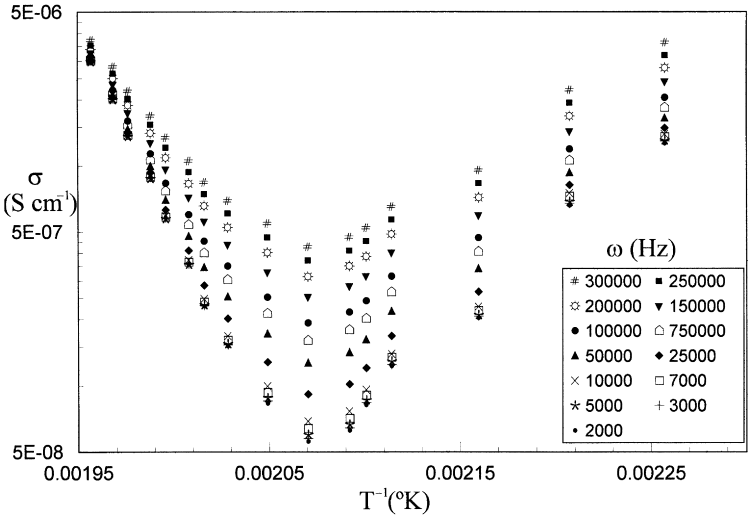

Figure 1 Ionic conductivity against inverse temperature for various frequencies

of the dielectric modulus $M(\omega) = M'(\omega) + M''(\omega)i$, defined by

$$M(\omega) = i\omega/\sigma(\omega). \quad (7)$$

The use of the dielectric modulus has the advantage of neglecting contributions to $M''(\omega)$ from electrode capacitances. Similarly, the impedance $Z(\omega) = Z'(\omega) - iZ''(\omega)$ is usually plotted in a complex impedance diagram Z' *versus* Z'' to obtain information about electrode contributions.

Data of conductivity against temperature are shown in *Figure 1* for several frequencies. As observed, an anomalous behaviour is seen at temperatures lower than a critical temperature (approximately 213°C, 486 K), where conductivity actually decreases with increasing temperature. Beyond this critical point, conductivity rises with temperature following a normal behaviour. The anomalous data may be ascribed to a morphological change occurring at lower temperatures than a critical temperature (T_s). Indeed, in the systems treated by Cardoso *et al.*[6], a sudden change in the slope of the conductivity *versus* temperature is observed at 488 K for polymer structures similar to the system treated here. Formation of aggregates and clusters inhibits the movements of dipoles responsible for the relaxation processes. Calorimetric measurements show the formation of a cluster phase as the sample is heated, and the presence of this new phase inhibits conductivity as the temperature is risen. It is well known[7,8] that cluster crystallinity inhibits conductivity by acting as potential barriers to conduction. For temperatures higher than T_s, the cluster phase is melted and conductivity starts to increase with temperature.

It is important to measure the a.c. conductivity in the appropriate temperature range to separate electrode polarization or blocking effects from the bulk conductivity. Indeed, in ion-containing polymers, d.c. conductivities are limited by electrode polarization or blocking effects. *Figure 2* shows ionic conductivity data in the 213–235°C temperature range. At the lowest frequencies, conductivity is not constant and this is caused by electrode polarization effects. D.c. conductivities are characterized by a frequency plateau and the transition into the frequency-dependent a.c. conductivity shifts to higher frequencies as the temperature is increased.

In ion-containing polymers, the dielectric behaviour at high temperatures is dominated by contributions of ionic conductivity, as in the case of ionenes[9]. It is usually encountered that dielectric data are characterized by the superposition of two processes: a conductivity contribution that produces an increase of both the real part ε' and the imaginary part ε'' of the dielectric function ε^* with decreasing frequency, and a relaxation process exhibiting a maximum in ε'' that shifts to higher frequencies with increasing temperature. In the zwitterionic polymers treated here, we do not observe the peak in ε'' within the frequency range available but, nevertheless, the increase in ε'' as frequency decreases due to the conductivity contribution is clearly manifested, as seen in *Figure 3*.

Empirical relationships are proposed for the conductivity and relaxation contributions contained in the ε'' data. The conductivity contribution to ε'' follows a power-law and the relaxation contribution is analysed using the Havriliak–Negami equation to account for the width and asymmetry of the relaxation process[10]. In the results presented here, it was found convenient to analyse the conductivity data directly in the framework of more fundamental models.

The complex dielectric function can be affected by electrode polarization. This causes deviations on the low frequency side of the Cole–Cole representation of the complex impedance. Deviations may become more pronounced with increasing temperature and hence increasing mobility and number of charge carriers. *Figure 4* shows the real (Z') and the imaginary (Z'') parts of the complex impedance (Z^*) plotted with frequency. Data are taken at several temperatures within 215–238°C range, which, although it is a narrow one, does correspond to the region where conductivity increases with temperature. Superposition is obtained after horizontal shifting of data reduced to an arbitrary temperature $T_0 = 225$°C using the a_T factor

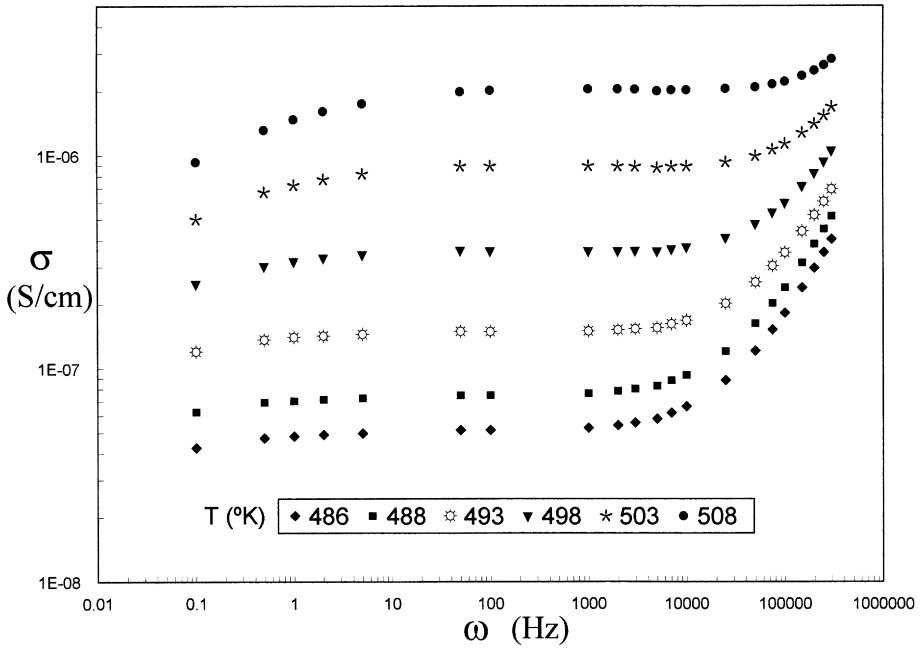

Figure 2 Ionic conductivity against frequency for various temperatures

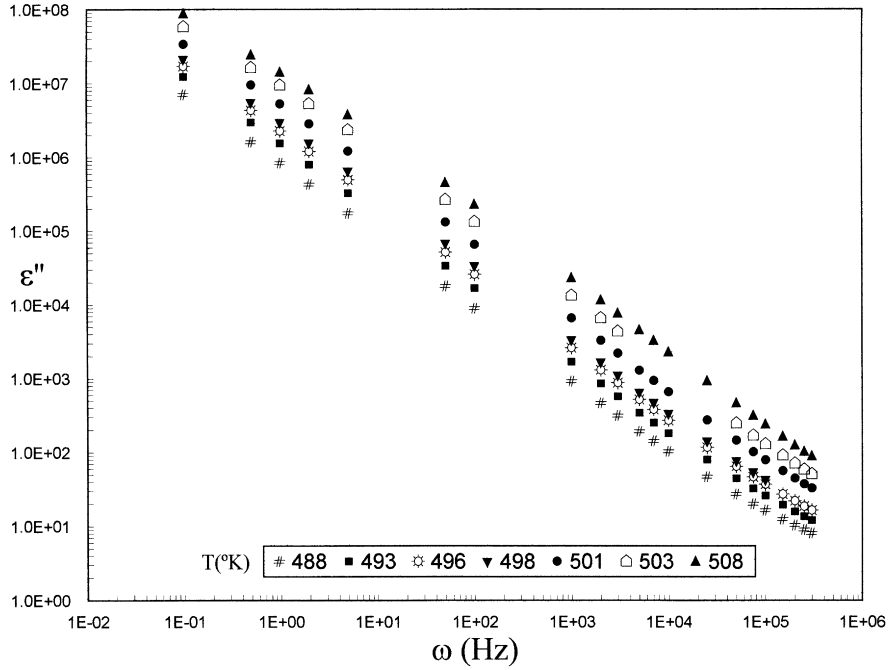

Figure 3 Imaginary part of the permittivity *versus* frequency for various temperatures

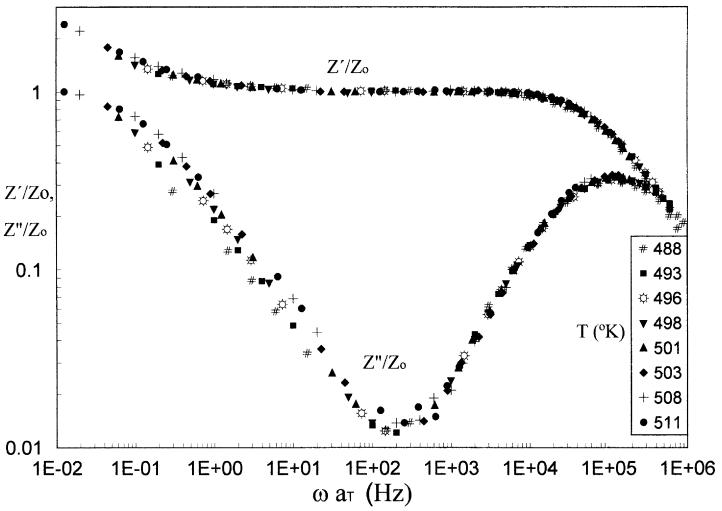

Figure 4 Reduced impedance (real and imaginary) curves *versus* non-dimensional frequency. Reference temperature is 498 K

defined as:

$$a_T = (\tau_Z)_T/(\tau_Z)_{T_0}, \tag{8}$$

were $(\tau_Z)_T$ is the impedance relaxation time (inverse frequency of the maximum of Z'') at temperature T referred to the relaxation time at the reference temperature T_o. It is clearly observed that the electrode contribution for values of ωa_T are lower than 10^2 in the Z'' curve. In the Cole–Cole representation (*Figure 5*), complex impedance arcs with depressed centres and deviations towards the low frequency side were found. This representation allows to ascribe the high-frequency semicircles to a conductivity contribution of the bulk sample, and the low-frequency arcs to an electrode polarization resistance.

Finally, *Figure 6* shows the superposed curves for several temperatures of the dielectric imaginary modulus (M'') against non-dimensional frequency. As observed, the modulus relaxation time, corresponding to the inverse frequency of the maximum in M'', has a lower magnitude than that of the impedance relaxation time ($\tau_M \approx 10^{-6}$ s, $\tau_Z \approx 10^{-5}$ s) shown in *Figure 4*, although the maximum in M'' cannot be determined accurately because it is not possible to obtain data at higher frequencies in the apparatus used. a_T values were evaluated by horizontal shifting of the curves reduced to 225°C as well. Arrhenius plots of impedance relaxation time (τ_Z) and modulus relaxation time (τ_M) represented by a_T reduced to the same temperature (225°C) are shown in *Figure 7*. Values do not differ largely, but activation energies are 282.8 kJ/mol for the impedance relaxation and 436 kJ/mol for the modulus relaxation.

DISCUSSION

From complex impedance data it is possible to elucidate the characteristics of the relaxation process. In fact, the Debye relaxation may be represented using the following

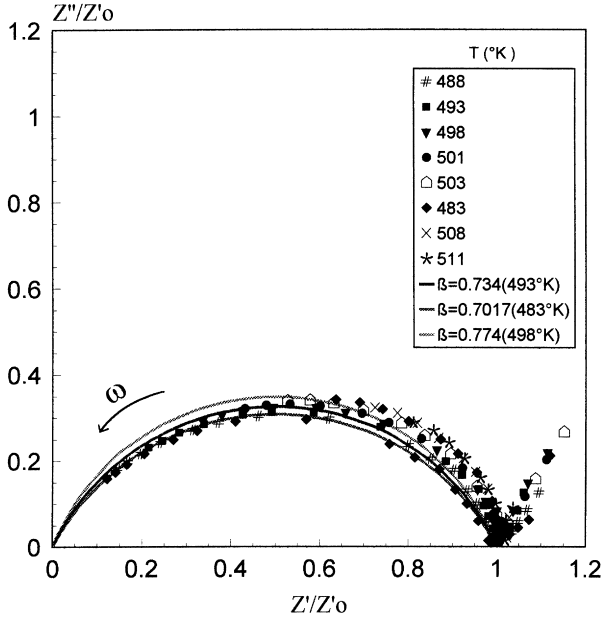

Figure 5 Cole–Cole plot of the impedance for several temperatures. Predictions of equation (11) are also shown for various values of the parameters

expression for Z^*:

$$Z* = \frac{R}{1 + i\omega\tau/r} - i\,\frac{R}{((r-1)/r)i\omega\tau}, \tag{9}$$

where $r = \varepsilon_S/\varepsilon_\infty$ (ε_S, ε_∞ are the static and the optical dielectric constants). As r is increased, the deviations from the semicircle are smaller. The relaxation process is thus a Debye relaxation with large relaxation ratio r, and in this case semicircles are found in both the impedance and dielectric planes. Similarly, a semicircular arc in the impedance plane is obtained in the case of a non-localized diffusion process of charge carriers[11]. This process is represented by a parallel RC circuit for the simplest case, which leads to:

$$Z* = \frac{R}{1 + i\omega\tau_Z}. \tag{10}$$

Therefore, if data follow a semicircle in the impedance plane, the behaviour can be ascribed to a strong Debye process or, alternatively, to a non-localized diffusion process. However, data in *Figure 5* do not strictly follow a Debye process, even at low temperatures where the arcs look symmetrical, because the semicircles centres are located below the Z' axis. In this case, the Cole–Cole expression fits the experimental data at 215°C (see values in *Figure 5*):

$$Z* = \frac{R}{1 + (i\omega\tau_Z)^\beta}. \tag{11}$$

where $\beta = 0.70$–0.77. Equation (11) indicates a superposition of Debye-like relaxation processes with a range of relaxation times symmetrically distributed about the main relaxation time τ_Z. For larger temperatures, the symmetry in the curves is lost and equation (11) does not predict the data appropriately, as shown in *Figure 5*. A more complicated empirical expression, i.e., the Havriliak–Negami expression, which may account for the asymmetry of the curves, would predict the experimental data better.

As mentioned, equation (10) may be expressed by a perfect semicircle in the complex impedance plane. This is the so called 'ideal conduction', which can be treated as an extremely strong Debye relaxation with τ_ε and τ_Y (dielectric and conductivity relaxation times) being infinitely large. Further in this case the d.c. conductivity becomes:

$$\sigma_0 = \frac{\varepsilon_\infty\varepsilon_0}{\tau_M} = \frac{\varepsilon_\infty\varepsilon_0}{\tau_Z}, \tag{12}$$

(which means that $\tau_M = \tau_Z$). Equation (12) has been used empirically by a number of authors[1,12–14]. It was further found that equation (12) holds when β is close to 1 and r is large[11,12]. In fact, the scaling suggested by equation (12) has been proved to be very satisfactory in predicting the conductivity for many oxide glasses[15]. In addition, both

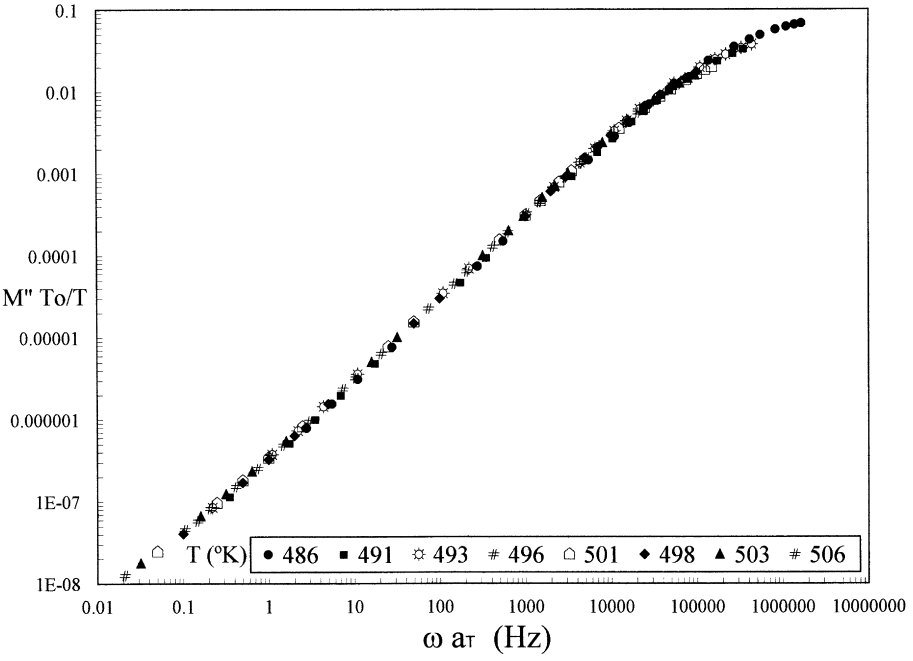

Figure 6 Imaginary part of the dielectric modulus *versus* non-dimensional frequency. Reference temperature is 498 K

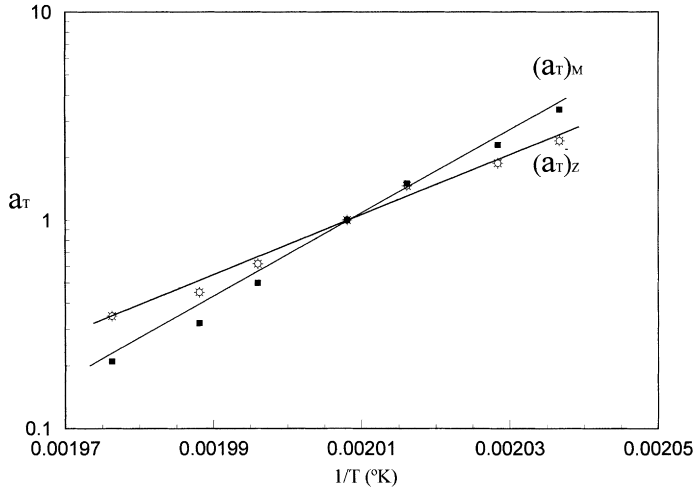

Figure 7 Shifting factor a_T (ratio of relaxation times) *versus* inverse temperature for the modulus $(a_T)_M$ and impedance $(a_T)_Z$

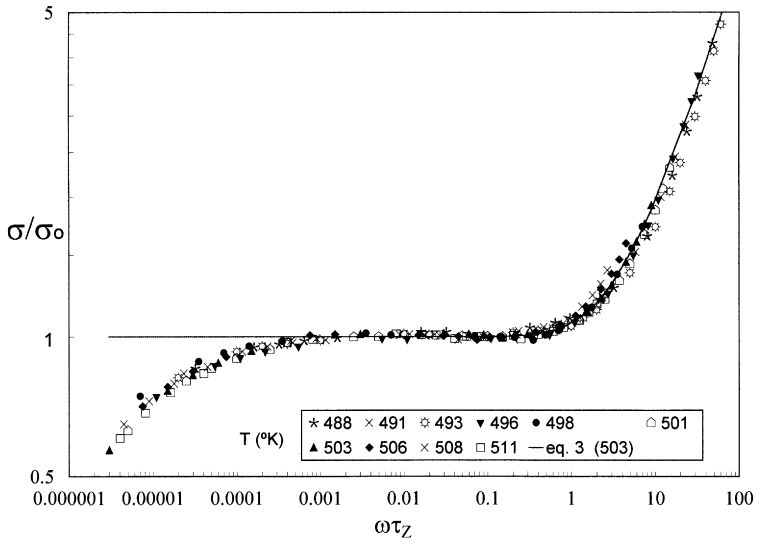

Figure 8 Reduced conductivity *versus* non-dimensional frequency using (τ_Z). Predictions of equation (3) are shown as a continuous line

the d.c. conductivity and relaxation times (τ_Z and τ_M) are expected to have the same activation energy for a thermally activated process since they depend strongly on temperature. However, activation energies (as observed in *Figure 7*) and magnitudes of the modulus and impedance relaxation times differ in this polymer.

The non-localized diffusion process generally dominates at low frequencies[16]. The non-localized conductivity (d.c. conductivity) represents a non-localized or long-range diffusion process. This conduction is accompanied by the rise in ε', ε'' at low frequencies (see *Figure 3*) in contrast to a localized relaxation process, which has a much smaller $\Delta\varepsilon$ and τ_ε. In fact, in a localized process, the maximum in ε'' is clearly observed within the frequency range of measurements, in contrast to the non-localized ε'' behaviour shown in *Figure 3*.

The modulus and impedance spectra shown in *Figures 4, and 6* can be represented by equivalent electrical circuits[17]. The response from the bulk sample would include a single capacitance, since a single polymeric phase with a corresponding conductivity is present. A pure capacitance C_e is added in series to represent the blocking electrodes. Let us propose an electric circuit which represent the bulk response of the sample, where a capacitance C_b is placed in parallel with a series of varying resistances, $R_1, R_2, \ldots R_n$, as shown below:

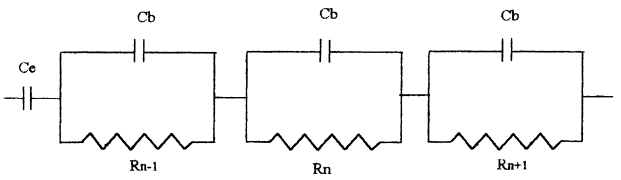

The response of such a circuit contains a single peak in the modulus spectrum, since this spectrum suppresses the low-frequency peak corresponding to the high-capacitance intergranular material. On the other hand, the impedance spectrum is composed of the cumulative or spectral contribution from *n* resistances (which reflect the individual resistances of the sample) with a global resistance represented by a single peak shifted to the lower frequencies. Now, let us further assume that the relaxation times τ_Z implied in the circuit, i.e.,

$$\tau_{Z_1} = R_1 C,\ \tau_{Z_2} = R_2 C, \ldots, \tau_{Z_n} = R_n C,$$

follow a box distribution of relaxation times. This means, in terms of a probability distribution, that

$$\tau_{Z_1}, \tau_{Z_2} \ldots \tau_{Z_n},$$

are equally likely, which is consistent with a process of delocalized diffusion within an equally probable distribution of free-energy barriers. As already described, the conductivity represented by the circuit above is given by equation (3). Data at several temperatures are shown in *Figure 8* with predictions from equation (3). Note the electrode contributions for values lower than 10 units of the non-dimensional frequency (using the impedance relaxation time). Also notice the power law region at high frequencies, with a slope that changes from 0.7 to 1.0, in agreement with predictions of the random free-energy barrier model.

For the dielectric loss, substituting equation (3) into equation (6), one finds:

$$\varepsilon''(\omega) = 2\Delta\varepsilon \left(\frac{\arctan(\omega\tau)}{[\ln\sqrt{1+(\omega\tau)^2}]^2 + [\arctan(\omega\tau)]^2} + \frac{1}{\omega\tau} \right) \tag{13}$$

where

$$\Delta\varepsilon = \sigma_0 \tau_\varepsilon / 2\varepsilon_0 \tag{14}$$

equation (13) implies a very broad loss peak with temperature-independent shape. However, in the present data the loss peak is absent at small frequencies and cannot be extracted from the electrode contributions. This is consistent with a large value of τ_ε characteristic of a delocalized conduction process described above. Consequently, quantitative agreement between equation (13) and data of *Figure 3*, where the peak is not present, is not found.As suggested by Dyre[2], plotting the reduced conductivity data against $\omega\tau$, where τ is given by equation (14) and considering the Curie law:

$$\Delta\varepsilon \propto \frac{1}{T} \tag{15}$$

reduced data gives the same superposition as in *Figure 8*. This scaling principle is consistent with the time–temperature superposition principle (i.e., the existence of a universal conductivity curve) which allows one to plot different experiments onto a master curve, as shown in *Figure 8*. Finally, it is worth pointing out that the agreement of data with equation (3) illustrates that the mechanism of long-range diffusion of charge carriers in this polymer is consistent with a process of delocalized diffusion within an equally probable distribution of free-energy barriers. However, in this case, the 'ideal conduction' mechanism is only approximately followed, since the modulus and impedance relaxation times are not equal neither their activation energies.

CONCLUSIONS

Conductivity behaviour of the zwitterionic polymers treated here as a function of frequency and temperature follows closely the predictions of the random free-energy barrier model with equally probable distribution of energy barriers. Along the available region where conductivity increases with temperature, data may be expressed as a master curve of the normalized conductivity *versus* dimensionless frequency. On the other hand, the dielectric loss peak is absent within the frequency range studied. The dielectric behaviour is hence dominated by the ionic conductivity.

Impedance curves clearly show the electrode contribution and the bulk response. At the lowest temperature these are symmetric and follow a Cole–Cole behaviour. For higher temperatures, the Z', Z'' representation shows non-symmetric semiarcs. Complex impedance data cannot simply be ascribed to a strong Debye process nor to a strictly 'ideal conduction' process, since deviations from semicircular arc in the impedance plane exist, and there are differences between activation energies and magnitudes of both the modulus and impedance relaxation times. Results only suggest an 'approximate ideal conduction' of the ion carriers, which is consistent with a large value of the dielectric relaxation time characteristic of delocalized conduction processes.

We are aware of the fact that the conductivity data presented can also be given an alternative theoretical interpretation. Indeed models such as those of Funke[18], Elliott[19], Dieterich[20], MacDonald[21] and other authors mentioned in the review paper by Hunt[22], are in many ways suitable to be applied to the conduction data, and suggest alternative explanations of the charge transport. Since the underlying mechanism of ionic conduction is still controversial, the choice of a single model with fundamental ingredients is henceforth justified.

ACKNOWLEDGEMENTS

We acknowledge the support from the 'Catedra Nivel II' from CONACYT.

REFERENCES

1. Dyre, J.C., *J. Non-Cryst. Solids*, 1986, **88**, 271.
2. Dyre, J.C., *J. Appl. Phys.*, 1989, **64**, 2456.
3. Montroll, E.W. and Weiss, G.H., *J. Math. Phys.*, 1965, **6**, 167.
4. Cardoso, J., Huanosta, A. and Manero, O., *Macromolecules*, 1991, **24**, 2890.
5. Cardoso, J., Huanosta, A., Montiel, R., González, L. and Manero, O., *J. Polym. Sci., Polym. Phys.*, 1994, **32**, 359.
6. Cardoso, J., Manrique, R., Albores, M. and Huanosta, A., *J. Polym. Sci., Polym. Phys.*, 1997, **35**, 479.
7. Sorensen, P.R. and Jacobsen, T., *Polym. Bull.*, 1983, **9**, 47.
8. Cardoso, J., Huanosta, A. and Manero, O., *Polym. Bull.*, 1991, **26**, 565.
9. Kremer, F., Dominguez, L., Meyer, W.H. and Wegner, G., *Polymer*, 1989, **30**, 2023.
10. Havriliak, S. and Negami, S., *Polymer*, 1967, **8**, 161.
11. Cao, W. and Gerhardt, R., *Solid State Ionics*, 1990, **42**, 213.
12. Isard, J.O., *J. Non-Cryst. Solids*, 1970, **4**, 357.
13. Tomozawa, M., *J. Non-Cryst. Solids*, 1979, **33**, 117.
14. Tomozawa, M., Cordaro, J. and Singh, M., *J. Mater. Sci.*, 1979, **14**, 1945.
15. Namikawa, H., *J. Non-Cryst. Solids*, 1975, **18**, 173.
16. Grant, E.A., *J. Appl. Phys.*, 1958, **29**, 76.
17. Hodge, Y.M., Ingram, M.D. and Nest, A.R., *J. Electroanal. Chem.*, 1976, **74**, 125.
18. Funke, K., *Ber. Bunsenges. Phys. Chem.*, 1989, **93**, 1197.
19. Elliot, S.R., *Solid State Ionics*, 1988, **27**, 131.
20. Dieterich, W., *Solid State Ionics*, 1990, **40**, 509.
21. MacDonald, J.R., *Solid State Ionics*, 1985, **15**, 159.
22. Hunt, A., *J. Non-Cryst. Solids*, 1993, **160**, 183.